nature materials

ARTICLES

PUBLISHED ONLINE: 16 NOVEMBER 2015 | DOI: 10.1038/NMAT4480

Thermodynamics of the hybrid interaction of hydrogen with palladium nanoparticles

Ronald Griessen[1]*, Nikolai Strohfeldt[2] and Harald Giessen[2]

Palladium–hydrogen is a prototypical metal–hydrogen system. It is therefore not at all surprising that a lot of attention has been devoted to the absorption and desorption of hydrogen in nanosized palladium particles. Several seminal articles on the interaction of H with Pd nanocubes and nanoparticles have recently been published. Although each article provides for the first time detailed data on specific aspects of hydrogen in nanoparticles, they individually do not contain enough information to draw firm conclusions about the involved mechanisms. Here, we show that the large body of data available so far in literature exhibits general patterns that lead to unambiguous conclusions about the processes involved in H absorption and desorption in Pd nanoparticles. On the basis of a remarkably robust scaling law for the hysteresis in absorption–desorption isotherms, we show that hydrogen absorption in palladium nanoparticles is consistent with a coherent interface model and is thus clearly different from bulk Pd behaviour. However, H desorption occurs fully coherently only for small nanoparticles (typically smaller than 50 nm) at temperatures sufficiently close to the critical temperature. For larger particles it is partially incoherent, as in bulk, where dilute α-PdH_x and high concentration β-PdH_x phases coexist.

Intercalation of small atoms in nanoparticles is relevant for important energy-related applications such as electrical batteries[1] and metal-hydrides[2] for electrical and hydrogen storage. In both systems the large lattice distortion[3] accompanying the absorption and desorption of the solutes plays an essential role in determining the performance of devices. Lattice distortions being long-ranged imply also that the thermodynamics of solute intercalation is inherently size-dependent[4]. This means specifically that the enthalpy and entropy of hydride formation, as well as the critical temperature T_c, depend on the size of nanoparticles. In many systems the technologically relevant temperatures are lower than T_c and, during absorption at a given hydrogen gas pressure, the metal–hydrogen system transforms from a dilute α-phase to a concentrated β-hydride. As a result of the magnitude of the lattice distortions accompanying this transformation (typically 15–20% relative volume increase per mole dissolved hydrogen in transition metals such as V, Nb, Ta and Pd) it is not a priori clear whether absorption (and desorption) of hydrogen occurs coherently or incoherently. In a coherent transformation the large spatial hydrogen concentration variations lead to a modulation of the host lattice without disrupting it, and consequently to significant coherency stresses and elastic energy contributions to the enthalpy (see Fig. 1). The elastic energy barrier accompanying coherency stresses is proportional to the sample volume and cannot be overcome by thermal fluctuations unless the particle is sufficiently small. During absorption the system is effectively locked in a metastable state until the increase in the chemical potential of the interstitials (which is proportional to the chemical potential of the surrounding H_2 molecules) is sufficiently high to overcome the macroscopic barrier. The transformation is then unlocked and spontaneous absorption starts[5,6]. Coexistence of two phases at thermodynamic equilibrium is then not possible and a large hysteresis between absorption and desorption pressures occurs at a given temperature. In an incoherent transformation, dislocations are readily created to minimize elastic stresses and incoherent β-phase precipitates nucleate and grow in the α-phase during absorption (see Fig. 1). The hysteresis is then largely reduced.

As measurements of H in Pd nanoparticles are very challenging, there is a great diversity in experimental techniques and samples[7–15]. The most extensive data have been obtained by Bardhan *et al.*[7] for dense ensembles of 14–110 nm nanocubes between 295 and 383 K. It was the first systematic attempt to investigate the size dependence of hydrogen absorption and desorption in ensembles of Pd nanocubes with narrow size distributions. The thermodynamics of hydrogenation was studied using luminescence as a proxy for the hydrogen content. The measured isotherms exhibit sloping plateaux and non-closing hysteresis loops. The first data on individual, colloidally synthesized and unconstrained nanocubes were obtained by Baldi *et al.*[8] by means of electron energy loss spectroscopy (EELS). Their isotherms for 13–29 nm nanocubes have flat plateaux but were measured only at one temperature (246 K). Very recently, Wadell[11] measured isotherms on ensembles of well-separated nanocubes with mean sizes of 22.5, 34.1 and 65.7 nm through Indirect NanoPlasmonic Sensing (INPS) and observed completely flat plateaux between 303 and 333 K. The methods used, namely, luminescence[7], EELS[8] and INPS[10,12] do not allow an absolute determination of the hydrogen concentration. Therefore, only the temperature dependence of the plateau pressures can be determined for a given size of nanocubes. Genuine pressure–composition isotherms (that is, isotherms in which the H concentration is actually measured) have been determined only for Pd clusters smaller than 7 nm by means of electrochemistry[13] and volumetry[14,15] and for 10 nm nanocubes[9] by volumetry at room temperature.

From measured absorption and desorption isotherms of their nanocube ensembles, Bardhan *et al.*[7] concluded that there are clear size-dependent trends in the thermodynamics. From a similarity of their measurements with Monte Carlo simulations based on the Ising model, they conclude these trends to be a consequence of nanoconfinement of a thermally driven, first-order phase transition,

[1]Faculty of Sciences, Division of Physics and Astronomy, VU University, De Boelelaan 1081, 1081 HV Amsterdam, The Netherlands. [2]4th Physics Institute and Research Center SCoPE, University of Stuttgart, Pfaffenwaldring 57, 70569 Stuttgart, Germany. *e-mail: r.p.griessen@vu.nl

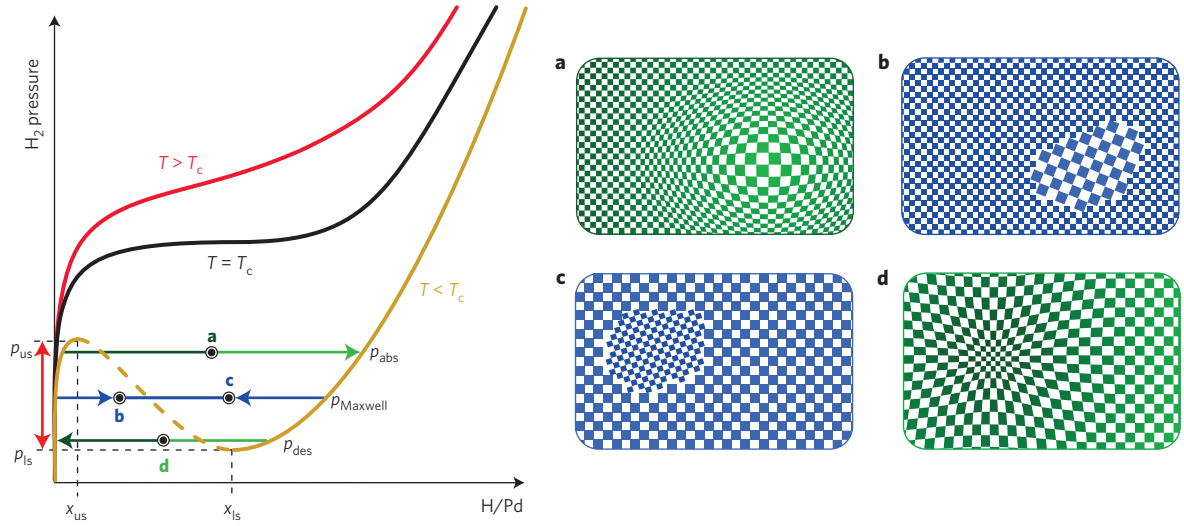

Figure 1 | Schematic pressure–composition isotherms at three different temperatures. The upper spinodal pressure p_{us} and the lower spinodal pressure p_{ls}, together with the corresponding spinodal concentrations x_{us} and x_{ls}, are indicated for the gold isotherm with $T < T_c$. The full-spinodal hysteresis is indicated with the red arrow. The horizontal blue line corresponds to the incoherent plateau pressure obtained by means of the Maxwell construction[29]. In bulk Pd H absorption occurs at $p_{abs} \approx p_{Maxwell}$ and an expanded β-PdH$_x$ phase nucleates incoherently in the dilute α-PdH$_x$ phase (**b**), whereas during desorption at $p_{des} \approx p_{Maxwell}$ the dilute α-PdH$_x$ nucleates and grows in the β-PdH$_x$ phase[20] (**c**). In the case where coherent absorption occurs at $p_{abs} \approx p_{us}$ (**a**) there is no coexistence of the α- and β-PdH$_x$ phases[5,6]. The gradient in H concentrations leads to continuous spatial variations of the lattice spacing. The same occurs during coherent desorption at $p_{des} \approx p_{ls}$ (**d**). The hysteresis is, according to Schwarz and Khachaturyan[6], comparable to the full-spinodal hysteresis. The black line corresponds to the critical isotherm at $T = T_c$ and the red line to a supercritical isotherm at $T > T_c$.

where α- and β-phases coexist incoherently, and that a large interfacial energy barrier is responsible for the opening of a hysteresis gap.

This is at variance with Baldi *et al.*[8], who found that, in single nanocubes at 246 K, surface stress due to excess hydrogen concentration near the surface of the nanocrystals accounts for the size dependence of the equilibrium absorption pressures and that absorption and desorption isotherms of individual nanocrystals are consistent with a coherent absorption process, without coexistence of two hydride phases. (Strictly speaking this conclusion is only applicable to H absorption as desorption could not reliably be measured with the used EELS technique.) In an earlier study Sachs *et al.*[16] suggested also that their data for 2–5 nm Pd clusters were consistent with the theory of Schwarz and Khachaturyan[5,6] for open, coherent two-phase systems. (Sachs *et al.* attributed erroneously to the molar volume v_0 of Pd (1.47×10^{-29} m^3) in equation (18) of ref. 5 a value that is equal to the partial molar volume (2.607×10^{-30} m^3) of hydrogen in palladium.) Evidence of the role of subsurface sites was also found in very small Pd clusters[10,13,14].

Although all these pioneering works have a fragmentary character (see Supplementary Fig. 1), we show that there are robust underlying patterns in the existing data. To put them into evidence, we consider here the crucial aspects of enthalpy–entropy compensation, absorption and desorption plateau pressures at room temperature, and isotherm hysteresis[17].

Enthalpy–entropy compensation

A collection of enthalpies, ΔH, and entropies, ΔS, of hydrogen absorption and desorption in Pd nanoparticles[7,11,12,15], a freestanding film[18] and bulk Pd[19,20] is shown in Fig. 2. There is a remarkably linear correlation between the measured ΔH and ΔS for samples of widely different sizes. The correlation is especially well obeyed for the desorption data. There is, however, no clear trend with particle size, Bardhan *et al.*'s[7] data being on the less negative ΔH side, whereas the Wadell[11] data obtained from measurements on the same type of nanocubes are on the more negative side. The origin of the ΔH–ΔS correlation is most likely related to the fact that the isotherms in ref. 7 exhibit strongly sloping plateaux and, in the smaller nanocubes, non-closing hysteresis loops (see Supplementary Section 3). Wadell[11] found, on the other hand, flat plateaux, but his data are restricted to the narrow temperature range of 303–333 K. In both cases, the conversion of absorption and desorption pressures into the thermodynamic parameters ΔH and ΔS is bound to be tricky (see Supplementary Sections 2 and 5). This can be demonstrated in the following way. A perfectly linear ΔH–ΔS correlation implies that $\Delta H = T_{comp}\Delta S + C$, where T_{comp} and C are the same constants for all samples. The slope $\partial\Delta H/\partial\Delta S$ is the compensation temperature T_{comp}, at which all plateau pressures have the same value p_{comp}. This follows directly from the Van 't Hoff relation

$$\frac{1}{2}\ln p = \frac{\Delta H}{RT} - \frac{\Delta S}{R} \qquad (1)$$

where p is the hydrogen pressure, R the gas constant, and T the absolute temperature. At $T = T_{comp}$ the pressure $p_{comp} = \exp(2C/RT_{comp})$ is constant. The compensation temperatures obtained from Fig. 2 for hydrogen absorption ($T_{comp} = 284 \pm 12$ K) and desorption ($T_{comp} = 343 \pm 6$ K) fall well within the range of the measurement temperatures chosen in refs 7,10–12,15. We would expect thus that the plateau pressures near room temperature are essentially the same in all data. We will show below that this expectation is not correct.

Plateau pressures at room temperature

As many existing data have been obtained near room temperature we show in Fig. 3 the plateau pressures at 300 K. (The plateau pressures at 300 K are either taken directly from quoted measured values or calculated from quoted enthalpies and entropies by means of equation (1). The half filled circles in Fig. 3 are estimated from the data of ref. 8 on single Pd nanocubes of sizes between 13 and 29 nm at 246 K by taking $\Delta S = -47.5$ J K^{-1} molH^{-1} in equation (1) (see Fig. 2).) Despite the large variation in sample

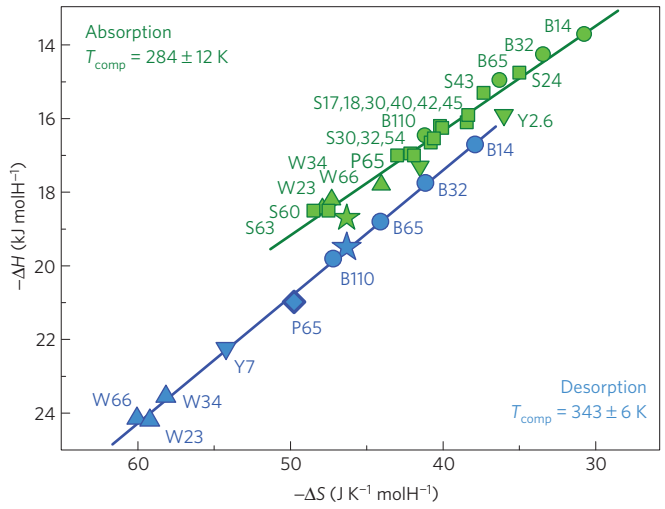

Figure 2 | Enthalpy–entropy correlation for H absorption and desorption in nanosized Pd particles. The labels are as follows: B14–B110 are for nanocubes from Bardhan *et al.*[7], W23–W66 are for the 22.5, 34.1 and 65.7 nm nanocubes from Wadell[11], Y2.6 and Y7 from Yamauchi *et al.*[15], and S17–S63 are for single nanocubes from Syrenova *et al.*[12]. Green symbols are for H absorption and blue symbols for H desorption. The number following the letter is the size of the particles in nm. The stars are for bulk Pd (ref. 19). For comparison data for a freestanding 65 nm film (P65) are also included[18]. The compensation temperatures T_{comp} are obtained from the equation $\Delta H = T_{comp}\Delta S + C$.

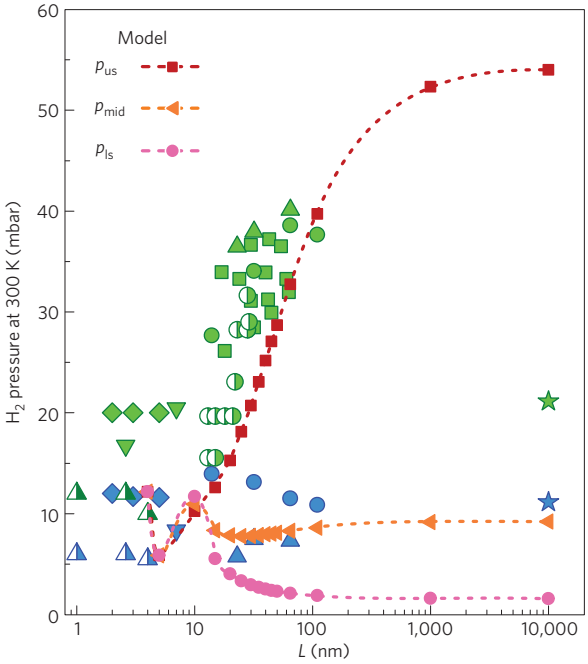

Figure 3 | Experimental and calculated plateau pressures at 300 K for H in Pd nanocubes and nanoparticles. The green symbols represent experimental data for hydrogen absorption and the blue symbols represent hydrogen desorption. Green and blue dots represent data from Bardhan *et al.*[7], triangles from Wadell[11], inverted triangles from Yamauchi *et al.*[15], half-filled triangles from Züttel *et al.*[13], diamonds from Sachs *et al.*[14], squares from Syrenova *et al.*[12], and stars from Lässer and Klatt[19]. Half-filled circles are evaluated from the absorption data of Baldi *et al.*[8]. The red squares (upper spinodal pressure p_{us}), pink dots (lower spinodal pressure p_{ls}) and orange triangles (midpressure p_{mid}) are calculated by means of the mean-field model described in the text and in Supplementary Information using the same parameters as in Fig. 5. The size L of the nanoparticles is plotted on a logarithmic scale to be able to cover the wide range of sizes ranging from 2 nm to bulk, which is arbitrarily set at 10^4 nm. The rapid variation of the calculated pressures for nanoparticles smaller than 10 nm marks the transition from core-dominated to surface-shell-dominated behaviour (see Supplementary Fig. 14). In a 9.7 nm nanocube the surface-shell and core volumes are equal (that is, $g = 0.5$).

preparation, size and shape, and the diversity of experimental techniques, there is a clear pattern emerging. The desorption pressures for nanostructures are essentially all equal to that of bulk Pd (refs 19–23). The absorption pressures of very small particles[13–15] (typically <8 nm) are also close to the absorption pressure of bulk Pd. In sharp contrast, however, the absorption pressure of nanocubes >8 nm increases markedly with increasing size L. This is bound to stop in large particles when hydrogen absorption breaks them into smaller crystallites. An estimate of the critical size of a nanoparticle is given in Supplementary Section 13.3. Noteworthy is that data obtained by INPS[11] on well-separated nanocubes are in good agreement with those derived from luminescence of dense nanocube ensembles[7].

The clear difference between the size dependence of absorption and desorption pressures indicates that the processes occurring during hydrogen absorption are fundamentally different from those during hydrogen desorption. The midpressure p_{mid}, defined as $\ln p_{mid} = 1/2(\ln p_{abs} + \ln p_{des})$ when considered in ref. 7, is therefore not a suitable parameter for discussing the intrinsic thermodynamics of nanocubes.

As desorption of hydrogen in bulk corresponds to that obtained by application of the Maxwell construction, that is, to a fully incoherent coexistence[24] of α-PdH$_x$ and β-PdH$_x$ phases, it is tempting to conclude that this does also happen in nanoparticles. However, the large hysteresis found experimentally in nanoparticles makes it then necessary to postulate that during absorption the concentration of H in α-PdH$_x$ increases until a pressure close to the upper spinodal pressure[25] p_{us} is reached (the corresponding concentration is x_{us}, see Fig. 1). These expectations are substantiated by considering the hysteresis measured during absorption–desorption cycles at constant temperature. The hysteresis is much better defined (see Supplementary Fig. 3) than pressure data and the corresponding Van 't Hoff plots, which all depend critically on the chosen concentration in the middle of the plateaux.

Isotherm hysteresis

The hysteresis is defined as the logarithm of the ratio of the absorption (p_{abs}) and desorption (p_{des}) plateau pressures. As the hysteresis vanishes at T_c, we expect a scaling law of the form (Supplementary Section 4)

$$\ln\left(\frac{p_{abs}(T,L)}{p_{des}(T,L)}\right) = f\left(\frac{T_c(L)}{T}\right) \qquad (2)$$

where $T_c(L)$ is the critical temperature of a nanoparticle of size L and f is a function with $f(1) = 0$. Figure 4 shows that the hysteresis of essentially all measured Pd nanocubes falls within the theoretical full-spinodal and 45%-spinodal hysteresis curves. This is completely different from the behaviour of bulk Pd (refs 19,21–23) (stars in Fig. 4). Data for a 50 nm Pd film[26] and a freestanding 65 nm film[18] exhibit a behaviour intermediate between nanocubes and bulk.

Starting from the simplest lattice gas model[27,28] (derivation in Supplementary Information), the full-spinodal line is

$$\ln\left(\frac{p_{us}}{p_{ls}}\right) = 8\frac{T_c}{T}z + 4\ln\left(\frac{1-z}{1+z}\right) \qquad (3)$$

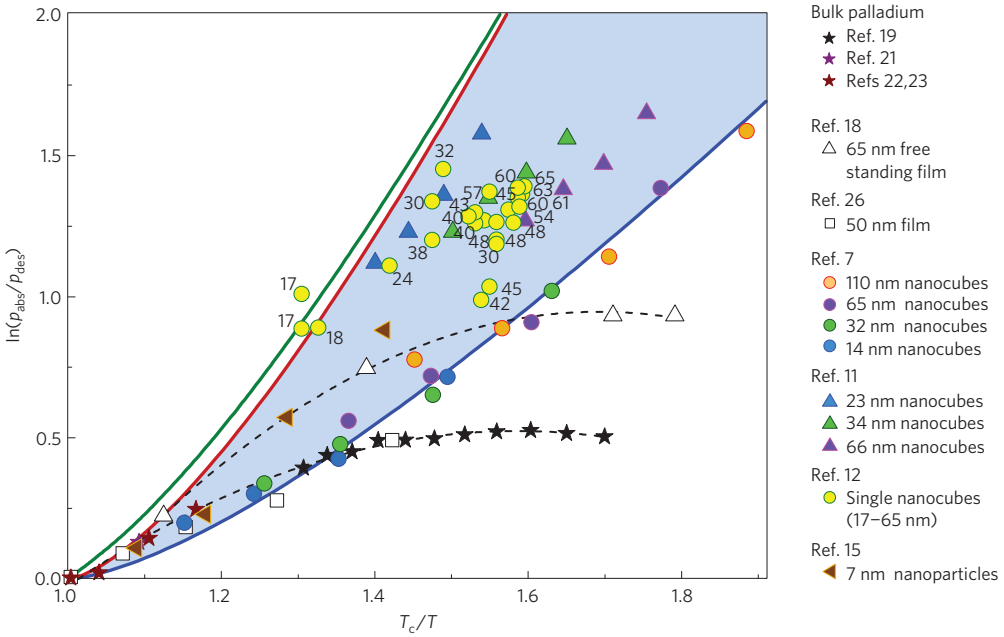

Figure 4 | Scaling law for the hysteresis. The hysteresis is plotted as a function of the inverse absolute temperature T normalized to the critical temperature T_c for Pd nanocubes[7,11,12,15] (the numbers next to the circles indicate the size L of the respective nanocubes), Pd films[18,26], and bulk Pd (refs 19,21–23). The determination of the critical temperatures is described in Supplementary Sections 5 and 6. For the nanocubes in refs 11 and 12, the T_c values are calculated by means of $T_c = 566\text{–}2{,}381/L$ (see Supplementary Fig. 7). The red line corresponds to the full-spinodal hysteresis obtained from equation (3), the blue line to 45%-spinodal and the green line is the full-spinodal hysteresis obtained from our fit (described in Supplementary Section 8) to the desorption data of bulk Pd critically analysed by Manchester and colleagues[20]. The black dashed lines through the bulk data and the freestanding film are a guide to the eye. The shaded blue area is the hysteresis region of our scaling law.

with $z = \sqrt{1 - T/T_c}$. This hysteresis (red curve in Fig. 4), which depends only on the ratio T/T_c, is the largest possible hysteresis in an absorption–desorption cycle (see Fig. 1). It is realized only if during hydrogen uptake the nanocube remains in a supersaturated α-PdH_x phase until the lower spinodal concentration x_{us} is reached and if during hydrogen release the nanocube remains in the concentrated β-PdH_x phase as long as $x > x_{ls}$. All the measured hystereses in Fig. 4 fall between the 100%-spinodal hysteresis (red curve) and the 45%-hysteresis (blue curve), defined as $0.45 \times \ln(p_{us}/p_{ls})$. This, together with the large difference between p_{abs} and p_{des} in Fig. 3, indicates that absorption occurs at $p_{abs} \approx p_{us}$, whereas desorption occurs at a pressure intermediate between the pressure $p_{Maxwell}$ (ref. 29) and the lower spinodal pressure p_{ls}. One expects, therefore, that hydrogen absorption proceeds coherently as predicted by Schwarz and Khachaturyan[5,6], whereas a fully incoherent coexistence of α- and β-PdH_x phases occurs during desorption as in bulk Pd samples[24]. There is, however, a clear trend for the hysteresis in Fig. 4 to tend towards a full-spinodal hysteresis in the limit $T_c/T \to 1$ (see also Supplementary Fig. 6). Interestingly, the data for 7 nm nanoparticles of Yamauchi *et al.*[15] and the nanocubes of Wadell[11] are systematically closer to full hysteresis than the nanocubes of Bardhan and colleagues[7]. It is unlikely that this difference is due to local heating effects (see Supplementary Section 7), as the scaling law turns out to be remarkably robust towards such effects. For the smallest nanoparticles, Fig. 3 indicates that there is still a small hysteresis. This is probably related to the used experimental method as the small width of the 'plateaux' at 300 K measured by Sachs *et al.*[14] indicates that T_c is close or below 300 K. The same applies to the isotherms measured on 2.7 and 5.3 nm Pd nanoparticles in ref. 10 and those on 2.6 nm nanoparticles in ref. 15.

One might at this point question the relevance of the simple expression in equation (3) for the hysteresis. To demonstrate that this expression is indeed relevant we have derived the full-spinodal hysteresis with a more general mean-field model including nonlinear H–H interactions (see Supplementary Section 8). As shown in Fig. 5a, this model reproduces accurately the bulk Pd isotherms over a wide range of temperatures, even well above the critical point $T_c = 566$ K. The measured desorption plateau pressures are very close to $p_{Maxwell}$ obtained by applying Maxwell's construction[29] to the calculated isotherms. Although the model involves a temperature-dependent enthalpy of solution, nonlinear effective H–H interactions, and a temperature- and concentration-dependent excess entropy, the calculated full-spinodal hysteresis is very close to that predicted by the simple equation (3) (see Fig. 4). This illustrates the usefulness of that simple expression.

Quantitative model for the isotherms of nanoparticles

The preceding conclusions are further substantiated by the quantitative comparison of experimental data and isotherms calculated by means of a mean-field model described in detail in Supplementary Section 9. The basic assumption of our model is similar to that of Weissmüller and Lemier[30,31], and Baldi and colleagues[8]. As proposed by Sachs *et al.*[14], hydrogen can be accommodated at subsurface sites in a surface shell of thickness t and at sites in the core of a nanoparticle (see Fig. 5b). The volume fraction g of surface-shell sites is defined as

$$g = \frac{V_{surf}}{V_{surf} + V_{core}} = 1 - \left(1 - \frac{2t}{L}\right)^3 \quad (4)$$

and the total concentration of hydrogen in the nanoparticle is

$$x_{total} = (1-g)x_{core} + g x_{surf} \quad (5)$$

where x_{surf} is the H concentration in the surface shell of volume V_{surf} and x_{core} is the H concentration in the nanoparticle core of

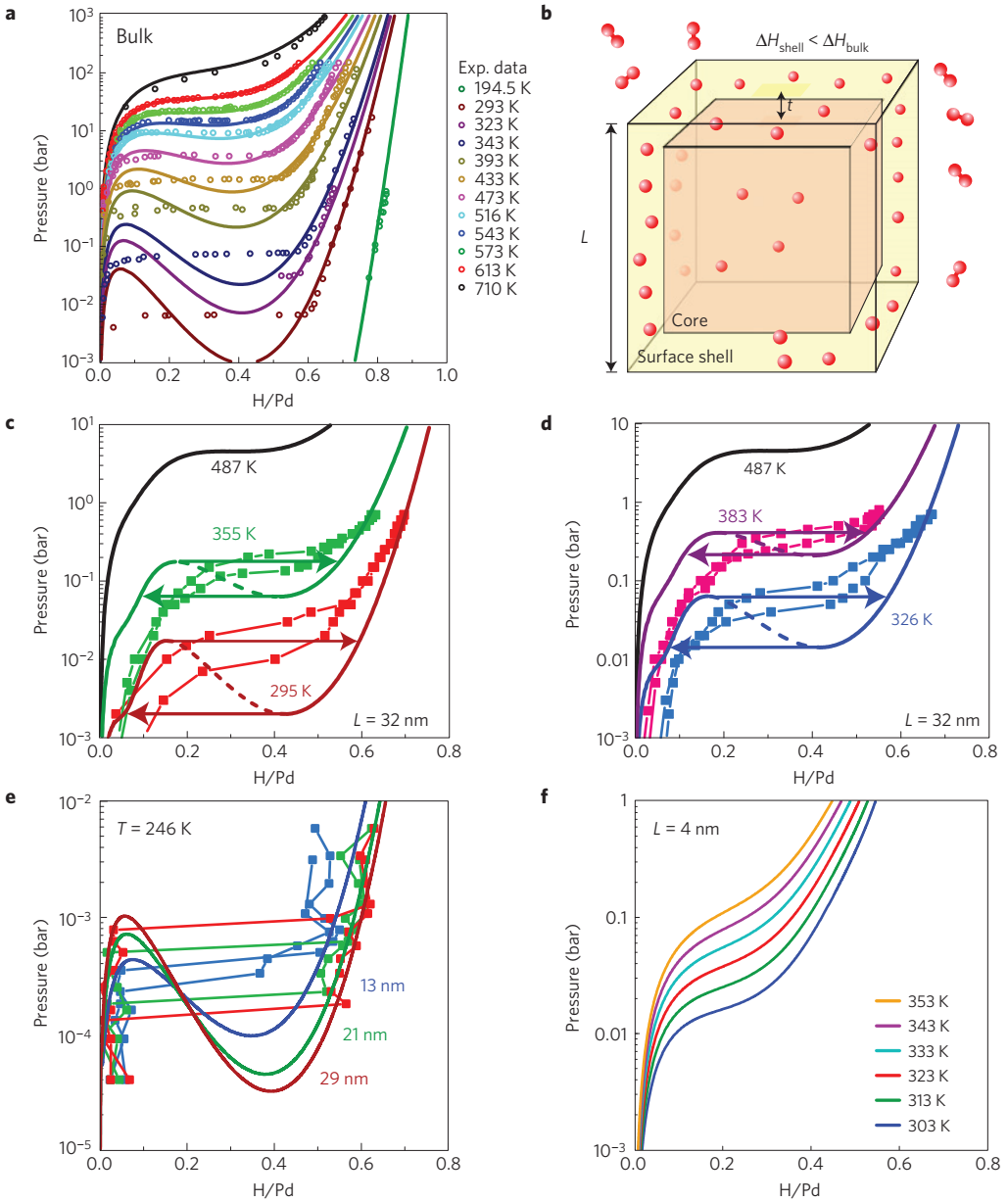

Figure 5 | Pressure–composition isotherms of various Pd samples, comparing model, and experimental data. a, Pressure–composition isotherms of bulk Pd compared to those calculated (coloured lines) with the mean-field lattice gas model described in Supplementary Information. The experimental data (coloured circles) taken from Manchester *et al.*[20] are for hydrogen desorption. **b**, Nanocube configuration used for the mean-field calculations of the isotherms in **c** to **f** (coloured lines). In **c** and **d**, as the hydrogen concentration cannot be determined from luminescence measurements the *x*-axis of the experimental isotherms of Bardhan *et al.*[7] for a 32 nm Pd nanocube are uniformly scaled for a better comparison with the model. The scaling factor is chosen so that the endpoint of every experimental loading curve coincides with the concentration H/Pd obtained from the model for the same pressure. The black lines correspond to the calculated critical isotherm at 487 K (see Supplementary Fig. 7a). **e**, Three representative isotherms measured by Baldi *et al.*[8] compared to the calculated isotherms. For this the EELS energy shifts are converted to a hydrogen concentration x_{core}, as EELS measures predominantly the core of the Pd nanocube. **f**, Pressure–composition isotherms calculated for a 4 nm Pd nanocube at temperatures between 303 and 353 K. The same parameters are used for all calculations in figures **c**–**f**, that is, an enthalpy of solution of −18,000 J molH^{-1} for the sites in a surface shell of thickness $t = 1$ nm, $\gamma = 0.5$, $u = 10{,}000$ J nm molH^{-1}, and $w = 1.6$ nm.

volume V_{core}. During H absorption, as the enthalpy of solution ΔH^{∞}_{surf} for surface-shell sites is more negative than that for core sites[31–33], ΔH^{∞}_{core}, the surface-shell H concentration x_{surf} is larger than x_{core}. This leads to H-dependent internal strains and, consequently, to H-dependent enthalpies in addition to the usual elastic and electronic effective H–H interactions, which are assumed to be the same as in bulk Pd. In addition, the model also takes into account surface tension[32,34] and clamping contributions[35] to the enthalpy of hydride formation[36].

Thermodynamic equilibrium between the surrounding H_2 gas at pressure p and temperature T, and H at interstitial sites in the surface shell and the core of the nanoparticle implies

$$\frac{1}{2}\ln p = \ln\left(\frac{x_{core}}{1-x_{core}}\right) + \frac{\Delta H_{core}(x_{core}, x_{surf}) + H_{elect}(x_{core}) + H_{st}}{RT} - \frac{\Delta S(x_{core})}{R} \quad (6)$$

for H at core sites and

$$\frac{1}{2}\ln p = \ln\left(\frac{x_{surf}}{1-x_{surf}}\right) + \frac{\Delta H_{surf}(x_{core},x_{surf}) + H_{elect}(x_{surf}) + H_{st}}{RT} - \frac{\Delta S(x_{surf})}{R} \quad (7)$$

at surface-shell sites. All enthalpies and entropies are given per molH. Owing to the elastic coupling between surface shell and core, the enthalpies ΔH_{surf} and ΔH_{core} depend on the H concentrations in both core and surface shell in the following way (see also Supplementary Section 9)

$$\Delta H_{core}(x_{core},x_{surf}) = \Delta H^{\infty}_{core} + (1-\gamma g)H_{elast}(x_{core},L) + \gamma g H_{elast}(x_{surf},L) \quad (8)$$

$$\Delta H_{surf}(x_{core},x_{surf}) = \Delta H^{\infty}_{surf} + (1-\gamma(1-g))H_{elast}(x_{surf},L) + \gamma(1-g)H_{elast}(x_{core},L) \quad (9)$$

For a spherical particle within linear elasticity theory one finds[4]

$$\gamma = \frac{2}{3}\left(\frac{1-2\nu}{1-\nu}\right) \quad (10)$$

where ν is the Poisson ratio. For Pd, $\nu = 0.39$ and $\gamma = 0.24$. As discussed by Fukai[37] and Feenstra *et al.*[38], γ is not necessarily given by equation (10) and can in practice be as large as 1. (In ref. 38, the value quoted for $\gamma = 0.15$ was obtained by assuming $\nu = 0.44$ for the Poisson ratio.) We consider γ as a free coupling parameter. The value in equation (10) corresponds to perfect elastic coupling. A vanishing γ corresponds to a complete decoupling between surface shell and core, and $\gamma = 1$ corresponds to an elastic enthalpy, which depends essentially only on the total concentration x_{total}. We assume furthermore that all the enthalpies H_{elast} (due to the attractive long range elastic H–H interaction), H_{elect} (due to the repulsive electronic H–H interaction) and ΔH^{∞}_{core} have the same concentration and temperature dependences as in bulk Pd. Explicit expressions for the enthalpies and entropies for bulk Pd are given in Supplementary Sections 8 and 9. To allow for partial clamping[35] by the substrate and/or an eventual surface contaminant or surfactant layer, and for a difference of elastic properties between core and surface shell, the attractive elastic H–H interaction enthalpy is allowed to be weakly size-dependent with $H_{elast}(x,L) = H_{elast}(x) \times (1-w/L)$, where w is an effective clamping thickness. The surface tension enthalpy term is taken as $H_{st} = u/L$, where $u = 4\sigma V_H$, with σ as the surface tension and V_H the hydrogen partial molar volume.

Pressure–composition isotherms are obtained from numerical calculations based on the coupled equations (6)–(9) and fitted to the data in refs 7,8,10. As shown in Fig. 5c–e and Supplementary Information, good quantitative agreement with the measured pressure–composition isotherms in refs 7,8,10 and the critical temperatures in Supplementary Fig. 7a is obtained with $\Delta H^{\infty}_{surf} = -18{,}000\,\mathrm{J\,molH^{-1}}$, $\gamma = 0.5$, $t = 1\,\mathrm{nm}$, $u = 10{,}000\,\mathrm{J\,nm\,molH^{-1}}$, and $w = 1.6\,\mathrm{nm}$. As discussed in Supplementary Information, all these values are reasonable[39–41].

A common feature of the calculated isotherms in Fig. 5c–e and Supplementary Fig. 11 is that the absorption plateau pressures are close to the upper spinodal pressure p_{us}, whereas the desorption pressures are intermediate between the incoherent (that is, Maxwell pressure $p_{Maxwell}$) and coherent desorption plateau pressures p_{ls}. We conclude that Pd nanocubes of intermediate size (~13 to ~110 nm) interact with hydrogen in a hybrid way: during H absorption the system remains in a supersaturated single phase until a pressure close to the upper spinodal pressure p_{us} is reached, after which it transforms coherently[5,6] (that is, without formation of dislocations) to the concentrated β-PdH$_x$ phase. Hydrogen absorption can thus be described by the theory of Schwarz and Khachaturyan[6]. Hydrogen desorption, on the other hand, occurs as if some of the coherency stresses built up during absorption have been released. Several hydrogen absorption–desorption scenarios are described in Supplementary Information. In particular, we show that if, during absorption, surface-shell–core coherency is maintained and no misfit dislocations are generated in the core, then H desorption remains coherent (see Supplementary Fig. 15), resulting in a full-spinodal hysteresis. In small particles, even when no dislocations are generated in the core, a reduced hysteresis can occur if the surface-shell–core elastic coupling is modified during absorption. This scenario leads to an 80%-hysteresis (Supplementary Fig. 16) that is consistent with the Syrenova *et al.*[12], Yamauchi *et al.*[15], and Wadell[11] data in Fig. 4. This scenario is also consistent with the observation that the crystallinity of the core of the nanocubes investigated in ref. 8 is preserved after several absorption and desorption cycles (A. Baldi, personal communication). Especially, near the corners and edges of the nanocubes, we expect a stress release mechanism similar to that observed in epitaxial YH$_x$ films to occur[42,43]. One possible modification might be that the larger lattice spacing of the hydrogen-loaded surface shell (compared to the core) is accommodated by allowing the surface shell to generate protrusions along the edges of the nanocube similar to the reversible edge generation observed in epitaxial YH$_x$ films[42,43]. This is more likely to happen at the surface of a cube than of a sphere, as the cube edges are clearly structurally different from the faces.

These conclusions break down as soon as dislocations are generated in the core. According to ref. 8 this occurs in nanocubes >35 nm. This estimate is, however, probably too low and should also be temperature-dependent, as discussed in Supplementary Section 13.3. A confirmation of the existence of a critical size follows from Supplementary Fig. 20, in which single nanocube data of Syrenova *et al.*[12] are compared to our calculated hysteresis.

Our model is also consistent with the data of Wadell *et al.*[10] for very small nanoparticles. The isotherms calculated for a 4 nm Pd nanoparticle at 303–353 K do not exhibit plateaux as the calculated critical temperature is 260 K (see Supplementary Fig. 7b). This explains why the enthalpies and entropies measured on 2.7 and 5.3 nm nanocubes are essentially the same for hydrogen absorption and desorption (see Fig. 4 in ref. 10).

We conclude that the model described in our work reproduces all the essential features of the thermodynamics of H in Pd nanoparticles over a wide range of sizes (from a few nm up to hundreds of nm) as long as no dislocations are generated in the core of the particles[44]. The value of the present investigation is primarily fundamental in the sense that it provides a consistent interpretation of the thermodynamics of H in Pd nanoparticles in particular, and of hydrogen in nanoparticles in general. Our framework is also relevant for other metal–hydrogen nanoparticle systems[45,46] (for example, YH$_x$, MgH$_x$) that have recently gained interest in the context of phase-change materials and active plasmonics.

Received 28 March 2015; accepted 12 October 2015; published online 16 November 2015

References

1. Armand, M. & Tarascon, J.-M. Building better batteries. *Nature* **451,** 652–657 (2008).
2. Pundt, A. Hydrogen in nano-sized metals. *Adv. Eng. Mater.* **6,** 11–21 (2004).
3. Griessen, R. & Feenstra, R. Volume changes during hydrogen absorption in metals. *J. Phys. F* **15,** 1013–1019 (1985).
4. Alefeld, G. Phase transitions of hydrogen in metals due to elastic interaction. *Ber. Bunsengesells. Phys. Chem.* **76,** 746–755 (1972).

5. Schwarz, R. B. & Khachaturyan, A. G. Thermodynamics of open two-phase systems with coherent interfaces. *Phys. Rev. Lett.* **74,** 2523–2526 (1995).
6. Schwarz, R. B. & Khachaturyan, A. G. Thermodynamics of open two-phase systems with coherent interfaces: Application to metal-hydrogen systems. *Acta Mater.* **54,** 313–323 (2006).
7. Bardhan, R. *et al.* Uncovering the intrinsic size dependence of hydriding phase transformations in nanocrystals. *Nature Mater.* **12,** 905–912 (2013).
8. Baldi, A., Narayan, T. C., Koh, A. L. & Dionne, J. A. *In situ* detection of hydrogen-induced phase transitions in individual palladium nanocrystals. *Nature Mater.* **13,** 1143–1148 (2014).
9. Li, G. *et al.* Hydrogen storage in Pd nanocrystals covered with a metal-organic framework. *Nature Mater.* **13,** 802–806 (2014).
10. Wadell, C. *et al.* Thermodynamics of hydride formation and decomposition in supported sub-10 nm Pd nanoparticles of different sizes. *Chem. Phys. Lett.* **603,** 75–81 (2014).
11. Wadell, C. *Plasmonic Nanostructures for Optical Absorption Engineering and Hydrogen Sensing* PhD thesis, Chalmers Univ. Technology, Sweden (2015).
12. Syrenova, S. *et al.* Hydride formation thermodynamics and hysteresis in individual Pd nanocrystals with different size and shape. *Nature Mater.* http://dx.doi.org/10.1038/nmat4409 (2015).
13. Züttel, A. *et al.* Thermodynamic aspects of the interaction of hydrogen with Pd clusters. *Appl. Surf. Sci.* **162,** 571–575 (2000).
14. Sachs, C. *et al.* Solubility of hydrogen in single-sized palladium clusters. *Phys. Rev. B* **64,** 075408 (2001).
15. Yamauchi, M., Ikeda, R., Kitagawa, H. & Takata, M. Nanosize effects on hydrogen storage in palladium. *J. Phys. Chem. C* **112,** 3294–3299 (2008).
16. Sachs, C. *et al.* Solubility of hydrogen in single-sized palladium clusters. *Phys. Rev. B* **64,** 075408 (2001).
17. Pundt, A. & Kirchheim, R. HYDROGEN IN METALS: Microstructural aspects. *Annu. Rev. Mater. Res.* **36,** 555–608 (2006).
18. Pivak, Y. *et al.* Effect of the substrate on the thermodynamic properties of PdH_x films studied by hydrogenography. *Scr. Mater.* **60,** 348–351 (2009).
19. Lässer, R. & Klatt, K. H. Solubility of hydrogen isotopes in palladium. *Phys. Rev. B* **28,** 748–758 (1983).
20. Manchester, F. D. *Phase Diagrams of Binary Hydrogen Alloys* (ASM International, 2000).
21. Picard, C., Kleppa, O. J. & Boureau, G. A thermodynamic study of the palladium–hydrogen system at 245–352 °C and at pressures up to 34 atm. *J. Chem. Phys.* **69,** 5549–5556 (1978).
22. de Ribaupierre, Y. & Manchester, F. D. Experimental study of the critical-point behaviour of the hydrogen in palladium system. I. Lattice gas aspects. *J. Phys. C* **7,** 2126–2139 (1974).
23. de Ribaupierre, Y. & Manchester, F. D. Experimental study of the critical-point behaviour of the hydrogen in palladium system. III. Spinodal curves and isotherm relations. *J. Phys. C* **8,** 1339–1348 (1975).
24. Wicke, E. & Blaurock, J. New experiments on and interpretations of hysteresis effects of Pd-D_2 and Pd-H_2. *J. Less-Common Met.* **130,** 351–363 (1987).
25. Haasen, P. & Mordike, B. L. *Physical Metallurgy* (Cambridge Univ. Press, 1996).
26. Feenstra, R., De Groot, D. G., Rector, J. H., Salomons, E. & Griessen, R. Gravimetrical determination of pressure–composition isotherms of thin PdH_c films. *J. Phys. F* **16,** 1953–1963 (1986).
27. Alefeld, G. *et al.* in *Hydrogen in Metals II: Application-Oriented Properties* Vol. 29 (eds Alefeld, G. & Völkl, J.) 1–387 (Springer, 1978).
28. Griessen, R. & Riesterer, T. in *Hydrogen in Intermetallic Compounds I: Electronic, Thermodynamic, and Crystallographic Properties, Preparation* Vol. 63 (ed. Schlapbach, L.) 219–284 (Springer, 1988).
29. Maxwell, J. C. On the dynamical evidence of the molecular constitution of bodies. *Nature* **11,** 357–359 (1875).
30. Weissmüller, J. & Lemier, C. On the size dependence of the critical point of nanoscale interstitial solid solutions. *Philos. Mag. Lett.* **80,** 411–418 (2000).
31. Lemier, C. & Weissmüller, J. Grain boundary segregation, stress and stretch: Effects on hydrogen absorption in nanocrystalline palladium. *Acta Mater.* **55,** 1241–1254 (2007).
32. Salomons, E., Griessen, R., De Groot, D. G. & Magerl, A. Surface tension and subsurface sites of metallic nanocrystals determined from H-absorption. *Europhys. Lett.* **5,** 449–454 (1988).
33. Dong, W., Ledentu, V., Sautet, P., Eichler, A. & Hafner, J. Hydrogen adsorption on palladium: A comparative theoretical study of different surfaces. *Surf. Sci.* **411,** 123–136 (1998).
34. Langhammer, C., Zhdanov, V. P., Zorić, I. & Kasemo, B. Size-dependent kinetics of hydriding and dehydriding of Pd nanoparticles. *Phys. Rev. Lett.* **104,** 135502 (2010).
35. Baldi, A., Gonzalez-Silveira, M., Palmisano, V., Dam, B. & Griessen, R. Destabilization of the Mg-H system through elastic constraints. *Phys. Rev. Lett.* **102,** 226102 (2009).
36. Bérubé, V., Radtke, G., Dresselhaus, M. & Chen, G. Size effects on the hydrogen storage properties of nanostructured metal hydrides: A review. *Int. J. Energy Res.* **31,** 637–663 (2007).
37. Fukai, Y. *The Metal-Hydrogen System: Basic Bulk Properties* (Springer Series in Materials Science, Springer, 2005).
38. Feenstra, R., Griessen, R. & DeGroot, D. G. Hydrogen induced lattice expansion and effective H–H interaction in single phase PdH. *J. Phys. F* **16,** 1933 (1986).
39. Wilde, M., Matsumoto, M., Fukutani, K. & Aruga, T. Depth-resolved analysis of subsurface hydrogen absorbed by Pd(100). *Surf. Sci.* **482–485,** 346–352 (2001).
40. Miedema, A. R. Surface energies of solid metals. *Z. Met.* **69,** 287–292 (1978).
41. Tyson, W. R. & Miller, W. A. Surface free energies of solid metals: Estimation from liquid surface tension measurements. *Surf. Sci.* **62,** 267–276 (1977).
42. Kerssemakers, J. W. J., Van der Molen, S. J., Koeman, N. J., Günther, R. & Griessen, R. Pixel switching of epitaxial $Pd/YH_x/CaF_2$ switchable mirrors. *Nature* **406,** 489–491 (2000).
43. Kerssemakers, J. W. J., Van der Molen, S. J., Günther, R., Dam, B. & Griessen, R. Local switching in epitaxial YH_x switchable mirrors. *Phys. Rev. B* **65,** 1–8 (2002).
44. Nörthemann, K. & Pundt, A. Coherent-to-semi-coherent transition of precipitates in niobium–hydrogen thin films. *Phys. Rev. B* **78,** 1–9 (2008).
45. Strohfeldt, N. *et al.* Yttrium hydride nanoantennas for active plasmonics. *Nano Lett.* **14,** 1140–1147 (2014).
46. Sterl, F. *et al.* Magnesium as novel material for active plasmonics in the visible wavelength range. *Nano Lett.* http://dx.doi.org/10.1021/acs.nanolett.5b03029 (2015).

Acknowledgements

We are grateful to J. Urban (Lawrence Berkeley National Laboratory) and A. Baldi (Stanford University) for providing us their original experimental data. We are especially grateful to C. Langhammer, C. Wadell and S. Syrenova (Chalmers University, Gothenburg) for making available pressure–composition isotherms of nanocube ensembles before publication. We also acknowledge enlightening discussions with A. Baldi, S. Syrenova and A. Pundt (University of Göttingen). R.G. was supported by an MPI guest professorship at University of Stuttgart and the MPI for Solid State Research. N.S. and H.G. were supported by the Deutsche Forschungsgemeinschaft (SPP1391, FOR730 and GI 269/11-1), by the Bundesministerium für Bildung und Forschung (13N9048 and 13N10146), by ERC Advanced Grant COMPLEXPLAS, by the Baden-Württemberg Stiftung (Spitzenforschung II) and by the Ministerium für Wissenschaft, Forschung und Kunst Baden-Württemberg (Az: 7533-7-11.6-8).

Author contributions

R.G. developed the theoretical framework for the enthalpy–entropy correlation and the hysteresis scaling law. N.S. developed the numerical method to calculate the pressure–composition isotherms of nanoparticles consisting of elastically coupled surface shell and core. H.G. coordinated the project. All authors contributed to the writing of the manuscript.

Additional information

Supplementary information is available in the online version of the paper. Reprints and permissions information is available online at www.nature.com/reprints. Correspondence and requests for materials should be addressed to R.G.

Competing financial interests

The authors declare no competing financial interests.